

Observation of isolated high- E_T photons in deep inelastic scattering

ZEUS Collaboration

Abstract

First measurements of cross sections for isolated prompt photon production in deep inelastic ep scattering have been made using the ZEUS detector at the HERA electron-proton collider using an integrated luminosity of 121 pb^{-1} . A signal for isolated photons in the transverse energy and rapidity ranges $5 < E_T^\gamma < 10 \text{ GeV}$ and $-0.7 < \eta^\gamma < 0.9$ was observed for virtualities of the exchanged photon of $Q^2 > 35 \text{ GeV}^2$. Cross sections are presented for inclusive prompt photons and for those accompanied by a single jet in the range $E_T^{\text{jet}} \geq 6 \text{ GeV}$ and $-1.5 \leq \eta^{\text{jet}} < 1.8$. Calculations at order $\alpha^3\alpha_s$ describe the data reasonably well.

The ZEUS Collaboration

S. Chekanov, M. Derrick, D. Krakauer, J.H. Loizides¹, S. Magill, S. Miglioranzi¹, B. Musgrave, J. Repond, R. Yoshida

Argonne National Laboratory, Argonne, Illinois 60439-4815, USA ⁿ

M.C.K. Mattingly

Andrews University, Berrien Springs, Michigan 49104-0380, USA

P. Antonioli, G. Bari, M. Basile, L. Bellagamba, D. Boscherini, A. Bruni, G. Bruni, G. Cara Romeo, L. Cifarelli, F. Cindolo, A. Contin, M. Corradi, S. De Pasquale, P. Giusti, G. Iacobucci, A. Margotti, A. Montanari, R. Nania, F. Palmonari, A. Pesci, G. Sartorelli, A. Zichichi

University and INFN Bologna, Bologna, Italy ^e

G. Aghuzumtsyan, D. Bartsch, I. Brock, S. Goers, H. Hartmann, E. Hilger, P. Irrgang, H.-P. Jakob, O. Kind, U. Meyer, E. Paul², J. Rautenberg, R. Renner, A. Stifutkin, J. Tandler³, K.C. Voss, M. Wang

Physikalisches Institut der Universität Bonn, Bonn, Germany ^b

D.S. Bailey⁴, N.H. Brook, J.E. Cole, G.P. Heath, T. Namsoo, S. Robins, M. Wing
H.H. Wills Physics Laboratory, University of Bristol, Bristol, United Kingdom ^m

M. Capua, A. Mastroberardino, M. Schioppa, G. Susinno

Calabria University, Physics Department and INFN, Cosenza, Italy ^e

J.Y. Kim, Y.K. Kim, J.H. Lee, I.T. Lim, M.Y. Pac⁵

Chonnam National University, Kwangju, Korea ^g

A. Caldwell⁶, M. Helbich, X. Liu, B. Mellado, Y. Ning, S. Paganis, Z. Ren, W.B. Schmidke, F. Sciulli

Nevis Laboratories, Columbia University, Irvington on Hudson, New York 10027 ^o

J. Chwastowski, A. Eskreys, J. Figiel, A. Galas, K. Olkiewicz, P. Stopa, L. Zawiejski
Institute of Nuclear Physics, Cracow, Poland ⁱ

L. Adamczyk, T. Bold, I. Grabowska-Bold⁷, D. Kisielewska, A.M. Kowal, M. Kowal, T. Kowalski, M. Przybycień, L. Suszycki, D. Szuba, J. Szuba⁸

Faculty of Physics and Nuclear Techniques, AGH-University of Science and Technology, Cracow, Poland ^p

A. Kotański⁹, W. Słomiński

Department of Physics, Jagellonian University, Cracow, Poland

V. Adler, U. Behrens, I. Bloch, K. Borras, V. Chiochia, D. Dannheim, G. Drews, J. Fourletova, U. Fricke, A. Geiser, P. Göttlicher¹⁰, O. Gutsche, T. Haas, W. Hain, S. Hillert¹¹, B. Kahle, U. Kötz, H. Kowalski¹², G. Kramberger, H. Labes, D. Lelas, H. Lim, B. Löhr, R. Mankel, I.-A. Melzer-Pellmann, C.N. Nguyen, D. Notz, A.E. Nuncio-Quiroz, A. Polini, A. Raval, L. Rurua, U. Schneekloth, U. Stösslein, G. Wolf, C. Youngman, W. Zeuner
Deutsches Elektronen-Synchrotron DESY, Hamburg, Germany

S. Schlenstedt
DESY Zeuthen, Zeuthen, Germany

G. Barbagli, E. Gallo, C. Genta, P. G. Pelfer
University and INFN, Florence, Italy^e

A. Bamberger, A. Benen, F. Karstens, D. Dobur, N.N. Vlasov
Fakultät für Physik der Universität Freiburg i.Br., Freiburg i.Br., Germany^b

M. Bell, P.J. Bussey, A.T. Doyle, J. Ferrando, J. Hamilton, S. Hanlon, D.H. Saxon, I.O. Skillicorn
Department of Physics and Astronomy, University of Glasgow, Glasgow, United Kingdom^m

I. Gialas
Department of Engineering in Management and Finance, Univ. of Aegean, Greece

T. Carli, T. Gosau, U. Holm, N. Krumnack, E. Lohrmann, M. Milite, H. Salehi, P. Schleper, T. Schörner-Sadenius, S. Stonjek¹¹, K. Wichmann, K. Wick, A. Ziegler, Ar. Ziegler
Hamburg University, Institute of Exp. Physics, Hamburg, Germany^b

C. Collins-Tooth, C. Foudas, R. Gonçalo¹³, K.R. Long, A.D. Tapper
Imperial College London, High Energy Nuclear Physics Group, London, United Kingdom^m

P. Cloth, D. Filges
Forschungszentrum Jülich, Institut für Kernphysik, Jülich, Germany

M. Kataoka¹⁴, K. Nagano, K. Tokushuku¹⁵, S. Yamada, Y. Yamazaki
Institute of Particle and Nuclear Studies, KEK, Tsukuba, Japan^f

A.N. Barakbaev, E.G. Boos, N.S. Pokrovskiy, B.O. Zhautykov
Institute of Physics and Technology of Ministry of Education and Science of Kazakhstan, Almaty, Kazakhstan

D. Son
Kyungpook National University, Center for High Energy Physics, Daegu, South Korea^g

K. Piotrkowski

Institut de Physique Nucléaire, Université Catholique de Louvain, Louvain-la-Neuve, Belgium

F. Barreiro, C. Glasman¹⁶, O. González, L. Labarga, J. del Peso, E. Tassi, J. Terrón, M. Vázquez, M. Zambrana

Departamento de Física Teórica, Universidad Autónoma de Madrid, Madrid, Spain^l

M. Barbi, F. Corriveau, S. Gliga, J. Lainesse, S. Padhi, D.G. Stairs, R. Walsh

Department of Physics, McGill University, Montréal, Québec, Canada H3A 2T8^a

T. Tsurugai

Meiji Gakuin University, Faculty of General Education, Yokohama, Japan^f

A. Antonov, P. Danilov, B.A. Dolgoshein, D. Gladkov, V. Sosnovtsev, S. Suchkov

Moscow Engineering Physics Institute, Moscow, Russia^j

R.K. Dementiev, P.F. Ermolov, I.I. Katkov, L.A. Khein, I.A. Korzhavina, V.A. Kuzmin, B.B. Levchenko¹⁷, O.Yu. Lukina, A.S. Proskuryakov, L.M. Shcheglova, S.A. Zotkin

Moscow State University, Institute of Nuclear Physics, Moscow, Russia^k

N. Coppola, S. Grijpink, E. Koffeman, P. Kooijman, E. Maddox, A. Pellegrino, S. Schagen, H. Tiecke, J.J. Velthuis, L. Wiggers, E. de Wolf

NIKHEF and University of Amsterdam, Amsterdam, Netherlands^h

N. Brümmner, B. Bylsma, L.S. Durkin, T.Y. Ling

Physics Department, Ohio State University, Columbus, Ohio 43210ⁿ

A.M. Cooper-Sarkar, A. Cottrell, R.C.E. Devenish, B. Foster, G. Grzelak, C. Gwenlan¹⁸, S. Patel, P.B. Straub, R. Walczak

Department of Physics, University of Oxford, Oxford United Kingdom^m

A. Bertolin, R. Brugnera, R. Carlin, F. Dal Corso, S. Dusini, A. Garfagnini, S. Limentani, A. Longhin, A. Parenti, M. Posocco, L. Stanco, M. Turcato

Dipartimento di Fisica dell'Università and INFN, Padova, Italy^e

E.A. Heaphy, F. Metlica, B.Y. Oh, J.J. Whitmore¹⁹

Department of Physics, Pennsylvania State University, University Park, Pennsylvania 16802^o

Y. Iga

Polytechnic University, Sagami-hara, Japan^f

G. D'Agostini, G. Marini, A. Nigro

Dipartimento di Fisica, Università 'La Sapienza' and INFN, Rome, Italy^e

C. Cormack²⁰, J.C. Hart, N.A. McCubbin
Rutherford Appleton Laboratory, Chilton, Didcot, Oxon, United Kingdom^m

C. Heusch
*University of California, Santa Cruz, California 95064, USA*ⁿ

I.H. Park
Department of Physics, Ewha Womans University, Seoul, Korea

N. Pavel
Fachbereich Physik der Universität-Gesamthochschule Siegen, Germany

H. Abramowicz, A. Gabareen, S. Kananov, A. Kreisel, A. Levy
Raymond and Beverly Sackler Faculty of Exact Sciences, School of Physics, Tel-Aviv University, Tel-Aviv, Israel^d

M. Kuze
Department of Physics, Tokyo Institute of Technology, Tokyo, Japan^f

T. Fusayasu, S. Kagawa, T. Kohno, T. Tawara, T. Yamashita
Department of Physics, University of Tokyo, Tokyo, Japan^f

R. Hamatsu, T. Hirose², M. Inuzuka, H. Kaji, S. Kitamura²¹, K. Matsuzawa
Tokyo Metropolitan University, Department of Physics, Tokyo, Japan^f

M.I. Ferrero, V. Monaco, R. Sacchi, A. Solano
Università di Torino and INFN, Torino, Italy^e

M. Arneodo, M. Ruspa
Università del Piemonte Orientale, Novara, and INFN, Torino, Italy^e

T. Koop, J.F. Martin, A. Mirea
Department of Physics, University of Toronto, Toronto, Ontario, Canada M5S 1A7^a

J.M. Butterworth²², R. Hall-Wilton, T.W. Jones, M.S. Lightwood, M.R. Sutton⁴, C. Targett-Adams
Physics and Astronomy Department, University College London, London, United Kingdom^m

J. Ciborowski²³, R. Ciesielski²⁴, P. Łuźniak²⁵, R.J. Nowak, J.M. Pawlak, J. Sztuk²⁶, T. Tymieniecka, A. Ukleja, J. Ukleja²⁷, A.F. Żarnecki
Warsaw University, Institute of Experimental Physics, Warsaw, Poland^q

M. Adamus, P. Plucinski
Institute for Nuclear Studies, Warsaw, Poland^q

Y. Eisenberg, D. Hochman, U. Karshon M. Riveline
Department of Particle Physics, Weizmann Institute, Rehovot, Israel^c

L.K. Gladilin²⁸, D. Kçira, S. Lammers, L. Li, D.D. Reeder, M. Rosin, A.A. Savin,
W.H. Smith

Department of Physics, University of Wisconsin, Madison, Wisconsin 53706, USA ⁿ

A. Deshpande, S. Dhawan

Department of Physics, Yale University, New Haven, Connecticut 06520-8121, USA ⁿ

S. Bhadra, C.D. Catterall, S. Fourletov, G. Hartner, S. Menary, M. Soares, J. Standage

Department of Physics, York University, Ontario, Canada M3J 1P3 ^a

- ¹ also affiliated with University College London, London, UK
- ² retired
- ³ self-employed
- ⁴ PPARC Advanced fellow
- ⁵ now at Dongshin University, Naju, Korea
- ⁶ now at Max-Planck-Institut für Physik, München, Germany
- ⁷ partly supported by Polish Ministry of Scientific Research and Information Technology, grant no. 2P03B 122 25
- ⁸ partly supp. by the Israel Sci. Found. and Min. of Sci., and Polish Min. of Scient. Res. and Inform. Techn., grant no.2P03B12625
- ⁹ supported by the Polish State Committee for Scientific Research, grant no. 2 P03B 09322
- ¹⁰ now at DESY group FEB
- ¹¹ now at Univ. of Oxford, Oxford/UK
- ¹² on leave of absence at Columbia Univ., Nevis Labs., N.Y., US A
- ¹³ now at Royal Holloway University of London, London, UK
- ¹⁴ also at Nara Women's University, Nara, Japan
- ¹⁵ also at University of Tokyo, Tokyo, Japan
- ¹⁶ Ramón y Cajal Fellow
- ¹⁷ partly supported by the Russian Foundation for Basic Research, grant 02-02-81023
- ¹⁸ PPARC Postdoctoral Research Fellow
- ¹⁹ on leave of absence at The National Science Foundation, Arlington, VA, USA
- ²⁰ now at Univ. of London, Queen Mary College, London, UK
- ²¹ present address: Tokyo Metropolitan University of Health Sciences, Tokyo 116-8551, Japan
- ²² also at University of Hamburg, Alexander von Humboldt Fellow
- ²³ also at Łódź University, Poland
- ²⁴ supported by the Polish State Committee for Scientific Research, grant no. 2 P03B 07222
- ²⁵ Łódź University, Poland
- ²⁶ Łódź University, Poland, supported by the KBN grant 2P03B12925
- ²⁷ supported by the KBN grant 2P03B12725
- ²⁸ on leave from MSU, partly supported by the Weizmann Institute via the U.S.-Israel BSF

- ^a supported by the Natural Sciences and Engineering Research Council of Canada (NSERC)
- ^b supported by the German Federal Ministry for Education and Research (BMBF), under contract numbers HZ1GUA 2, HZ1GUB 0, HZ1PDA 5, HZ1VFA 5
- ^c supported by the MINERVA Gesellschaft für Forschung GmbH, the Israel Science Foundation, the U.S.-Israel Binational Science Foundation and the Benozio Center for High Energy Physics
- ^d supported by the German-Israeli Foundation and the Israel Science Foundation
- ^e supported by the Italian National Institute for Nuclear Physics (INFN)
- ^f supported by the Japanese Ministry of Education, Culture, Sports, Science and Technology (MEXT) and its grants for Scientific Research
- ^g supported by the Korean Ministry of Education and Korea Science and Engineering Foundation
- ^h supported by the Netherlands Foundation for Research on Matter (FOM)
- ⁱ supported by the Polish State Committee for Scientific Research, grant no. 620/E-77/SPB/DESY/P-03/DZ 117/2003-2005
- ^j partially supported by the German Federal Ministry for Education and Research (BMBF)
- ^k partly supported by the Russian Ministry of Industry, Science and Technology through its grant for Scientific Research on High Energy Physics
- ^l supported by the Spanish Ministry of Education and Science through funds provided by CICYT
- ^m supported by the Particle Physics and Astronomy Research Council, UK
- ⁿ supported by the US Department of Energy
- ^o supported by the US National Science Foundation
- ^p supported by the Polish State Committee for Scientific Research, grant no. 112/E-356/SPUB/DESY/P-03/DZ 116/2003-2005, 2 P03B 13922
- ^q supported by the Polish State Committee for Scientific Research, grant no. 115/E-343/SPUB-M/DESY/P-03/DZ 121/2001-2002, 2 P03B 07022

1 Introduction

Isolated photons in the final state with high transverse momenta are a direct probe of the dynamics of hard subprocesses in high energy collisions, since these ‘prompt’ photons are largely insensitive to the effects of hadronisation. Prompt photons have been studied in a number of hadronic experiments. Early evidence for such processes came from the R806 experiment at the CERN ISR [1]. More recently, the CDF and DØ experiments at the Tevatron collider have performed a number of QCD tests using prompt photons [2–7]. In previous ZEUS publications, the production of prompt photons in photoproduction has been studied [8–10]. In the present letter, for the first time, prompt photon measurements in deep inelastic scattering (DIS) are reported, both inclusively and accompanied by jets. These processes test QCD in a new way by studying processes containing two different hard scales, Q^2 , the exchanged photon virtuality, and E_T^γ , the transverse energy of the emitted prompt photon.

Prompt photons are produced in DIS at lowest order in QCD, as shown in Fig. 1. These processes have been calculated to order $O(\alpha^3\alpha_s)$ by Gehrmann-DeRidder, Kramer and Spiesberger [11], including interference terms for initial- and final-state radiation from the electron. In contrast, leading-logarithm parton-shower Monte Carlo (MC) models do not naturally predict events with two hard scales.

In this letter, results are presented for the process $ep \rightarrow e\gamma X$, where X is anything, and for $ep \rightarrow e\gamma + \text{jet} + Y$, where Y does not contain further jets within the acceptance of the measurement. Comparisons are made to MC predictions and also to $O(\alpha^3\alpha_s)$ calculations for the photon-jet final state.

2 Experimental set-up and event selection

A data sample corresponding to an integrated luminosity of 121 pb^{-1} was used, taken between 1996 and 2000. This sample is the sum of 38 pb^{-1} of e^+p data taken at a centre-of-mass energy of 300 GeV and 68 pb^{-1} taken at 318 GeV, plus 16 pb^{-1} of e^-p data taken at 318 GeV. A single set of results is presented for this combined sample. The MC cross sections (see Section 3) differ by under 4% at the two centre-of-mass energies, well within the precision of these measurements. Differences between the cross-sections for e^+p and e^-p collisions are expected to be negligible [12].

A description of the ZEUS detector is given elsewhere [13]. Of particular importance in the present work are the uranium calorimeter (CAL) and the central tracking detector (CTD).

The CAL [14] has an angular coverage of 99.7% of 4π and is divided into three parts (FCAL, BCAL, RCAL), covering the angular ranges $2.6^\circ - 36.7^\circ$, $36.7^\circ - 129.1^\circ$ and $129.1^\circ - 176.2^\circ$, respectively¹. Each part consists of towers longitudinally subdivided into electromagnetic (EMC) and hadronic (HAC) cells. The electromagnetic section of the BCAL (BEMC) consists of cells of 23.3 cm length azimuthally, representing 1/32 of the full 360° , and width of 4.9 cm in the Z direction at its inner face, at a radius of 123.2 cm from the beam line. These cells have a projective geometry as viewed from the interaction point. The profile of the electromagnetic signals observed in clusters of cells in the BEMC discriminates between those originating from photons or electrons² and those originating from neutral-meson decays. The CAL energy resolutions, as measured under test-beam conditions, are $\sigma(E)/E = 0.18/\sqrt{E}$ for electromagnetic showers and $\sigma(E)/E = 0.35/\sqrt{E}$ for hadrons, with E in GeV.

The CTD [15] is a cylindrical drift chamber situated inside a superconducting solenoid. Using the tracking information from the CTD, the vertex of an event can be reconstructed with a resolution of 0.4 cm in Z and 0.1 cm in X, Y . In this analysis, the CTD tracks are used to reconstruct the event vertex, and are also used in the selection criteria for high- E_T photons.

The luminosity was determined from the rate of the bremsstrahlung process $ep \rightarrow e\gamma p$, where the high-energy photon was measured in a lead-scintillator calorimeter [16] located at $Z = -107\text{m}$.

The DIS events were selected online using a trigger based on energy deposits in the CAL consistent with a scattered electron. Offline, events which passed DIS cuts similar to those used in previous analyses [17] were selected. In addition a photon candidate was required. The value of Q^2 , as reconstructed from the final-state electron, was required to be above 35 GeV^2 . The energy of the scattered electron was required to be above 10 GeV and its polar angle in the range 139.8° to 171.9° , in order to be well measured in the RCAL and well separated from the photon candidate. Events were required to have a reconstructed vertex position within the range $|Z| < 40 \text{ cm}$ and $35 < \delta < 65 \text{ GeV}$, where $\delta = \sum_i E_i(1 - \cos \theta_i)$, E_i is the energy of the i th CAL cell, θ_i is its polar angle and the sum runs over all cells.

For the subset of events used in the photon-jet study, jets were reconstructed from CAL cells using a cone algorithm with radius 0.7 [18] in the laboratory frame. Corrections for energy losses, principally due to uninstrumented material in front of the CAL, were eval-

¹ The ZEUS coordinate system is a right-handed Cartesian system with the Z axis pointing in the proton beam direction, referred to as the ‘forward direction’, and the X axis pointing left towards the centre of HERA. The coordinate origin is at the nominal interaction point.

² Hereafter ‘electron’ refers both to electrons and positrons unless specified.

uated using MC simulated events, and were typically +(10-15)% for jets with measured energy above 6 GeV [10].

3 Monte Carlo event simulation

The MC programs PYTHIA 6.206 [19] and HERWIG 6.1 [20] were used to simulate prompt photon emission for the study of event-reconstruction efficiency. In both generators, the partonic processes are simulated using leading-order matrix elements, with the inclusion of initial- and final-state parton showers. Fragmentation into hadrons is performed using the Lund string model [21] in the case of PYTHIA, and a cluster model [22] in the case of HERWIG. The events generated using the PYTHIA and HERWIG programs were used to correct for detector and acceptance effects. The corrections provided by PYTHIA were used as default and those given by HERWIG were used to estimate the systematic uncertainties due to the treatment of the event dynamics and of parton showering and hadronisation. The detector response to photons and neutral mesons (π^0 and η) was simulated by using single-particle MC generated events.

The generated events were passed through the ZEUS detector and trigger simulation programs based on GEANT 3.13 [23]. They were reconstructed and analysed by the same programs as the data. The jet search was performed using the energy measured in the CAL cells in the same way as for the data. The same jet algorithm was also applied to the final-state particles.

To study the effects of electron radiation, simulations were made of deep inelastic scattering events using the HERACLES 4.6.1 [24] program with the DJANGO [25] interface to the MC generators that provide the hadronisation. The collinear radiative corrections were found to be small in the kinematic region of this analysis and were neglected.

4 Photon candidate selection

The identification of events containing an isolated prompt photon candidate follows closely the approach used in previous analyses [8–10]. Events were selected on the basis of an isolated photon candidate detected in the BCAL. The algorithm selected predominantly electromagnetic clusters of cells within a small angular cone. Initially, larger electromagnetic clusters than are typical of a single photon were accepted to estimate backgrounds. Use of shower shapes as a discriminant, as described below, allowed subtraction of the backgrounds due to π^0 and η production.

It was required that the reconstructed transverse energy of the cluster satisfied $E_T^\gamma > 5 \text{ GeV}$ and the pseudorapidity satisfied $-0.7 < \eta^\gamma < 0.9$. The cut $E_T^\gamma < 10 \text{ GeV}$ was imposed to ensure that the π^0 and η subtraction method was effective.

The photon candidate was well separated from the scattered electron. Monte Carlo simulations and $O(\alpha^3\alpha_s)$ calculations (see Section 6.2) show that for electrons in the range defined in Section 2, most photons radiated from the electron fall outside the prompt-photon acceptance used in this analysis, though they still give an important contribution to the cross section in the kinematic region of the measurement.

To reduce backgrounds, the photon-candidate cluster was required to be isolated by demanding $\Delta r > 0.2$, where $\Delta r = \sqrt{\Delta\phi^2 + \Delta\eta^2}$, the distance to the nearest reconstructed track in $\eta-\phi$ space. It was further required that $E_T^\gamma/E_T^{\text{cone}} > 0.9$, where E_T^{cone} is the energy within a cone in $\eta-\phi$ of radius 1.0 around the photon candidate. This energy isolation requirement suppresses the contribution from photon candidates produced within jets. Deeply virtual Compton scattering (DVCS) events were removed by demanding at least two tracks reconstructed in the CTD, since in DVCS the final state seen in the detector consists only of a photon and an electron which are well separated [26, 27].

The selected candidates were still dominated by neutral mesons, such as π^0 and η , which decay to photons. The single-photon signal was statistically extracted from the background using BEMC energy-cluster shapes. The first distribution considered was that of $\langle\delta Z\rangle$, where $\langle\delta Z\rangle = \Sigma(E_{\text{cell}}|Z_{\text{cell}} - \bar{Z}|)/\Sigma E_{\text{cell}}$. Here E_{cell} is the energy deposited in a BEMC cell, Z_{cell} is the cell number measured in the Z direction and \bar{Z} is the energy-weighted mean of Z_{cell} . Figure 2a shows the $\langle\delta Z\rangle$ distribution for data, together with a fit based on photon shower shapes and a simulation of single particles in the detector (π^0 and η). Clear peaks are visible at $\langle\delta Z\rangle \simeq 0.15$ due to single photons and $\langle\delta Z\rangle \simeq 0.5$ due to $\pi^0 \rightarrow \gamma\gamma$, as well as a tail due to the decays of heavier particles to two or more photons.

The photon shower shapes used were derived in two ways: from DVCS data [27], and from single-photon MC simulation. In Fig. 2, photons found in DVCS data events are shown. The results of the two shower-shape methods gave indistinguishable background subtractions and differed only by an overall scale factor of 5% on the acceptance of the prompt-photon signal. The DVCS method gave the higher acceptance, as the DVCS single-photon showers are slightly narrower than those from the MC showers. The MC method was used in this analysis, because of the higher statistics available. This allows rapidity and energy dependences of shower shapes to be modelled; a scale correction of 5% was then applied.

The η contribution was determined from a fit to the $\langle\delta Z\rangle$ distribution above 0.65. After removing candidates with $\langle\delta Z\rangle > 0.65$, the final background subtraction was performed using the variable f_{max} , defined as the ratio of the energy of the highest-energy cell in an

electromagnetic cluster to the total cluster energy. When incident on the BEMC, single photons form narrow clusters, with most of the energy going into only one cell, giving an f_{\max} distribution peaked close to unity. Because of the projective geometry of the BEMC, a photon entering at the boundary between two cells typically has $f_{\max} \simeq 0.5$. Thus the f_{\max} distribution for single photons peaks close to 1.0 and extends down to 0.5. In contrast, the neutral mesons decay to more than one photon, forming larger clusters in the BEMC. In each bin of a plotted physical quantity, events were divided into two classes, with high and low values of f_{\max} respectively. From the number of events in each class, as well as the ratios of the corresponding numbers for the f_{\max} distributions of the single-particle samples, the number of events in the given bin was evaluated [8].

A total of 1875 events with $\langle \delta Z \rangle < 0.65$ were selected, of which 877 have $f_{\max} > 0.75$, yielding a signal of 572 and a background of 1303 events. The fits and signal extraction procedure were repeated for each bin of each distribution.

Studies based on single-particle MC samples showed that the photon energy measured in the BCAL was on average less than the true value, owing to energy loss in the uninstrumented material in front of the BCAL. To compensate for this effect, a correction of typically 0.2 GeV was added to the photon energy [10].

5 Systematic uncertainties

The following sources of systematic uncertainty were investigated: variations of the nominal f_{\max} spectra for the photon affecting the signal extraction; change in the detector energy scale calibration by $\pm 3\%$, reflecting the overall energy scale uncertainty; and a change in the energy cut in both MC events and data by $\pm 10\%$ for photons. This last uncertainty is motivated by the r.m.s. differences between hadron-level generated and reconstructed energies. Also included as a systematic uncertainty is the difference in estimated acceptance between HERWIG and PYTHIA, which is mostly well below the statistical uncertainty. A change of $\pm 20\%$ in the hadronic energy cut for photon-jet events for both data and reconstructed Monte Carlo events, representing the r.m.s. difference between hadron-level and reconstructed jet energies was considered as an additional systematic uncertainty. The uncertainty of 2.2% on the luminosity measurement was neglected in the differential cross sections but included in the total cross sections.

The method used for background subtraction is more sensitive to the shape of the f_{\max} distribution of the background than to that of the signal. The background shape is relatively insensitive to the π^0/η ratio and hence the results using DVCS and MC photons are very similar. A study was made of the effect on the results of the fact that the fits fall below the data at high $\langle \delta Z \rangle$. This is due to events with large E_T^γ , where the contribution

of events with more than one π^0 with a multi- π^0 invariant mass above the η mass is likely to be important. A fit was made to the high- E_T^γ data excluding the region $\langle \delta Z \rangle > 1.0$. The change in the extracted signal was well below the statistical uncertainty in the bin.

6 Results

6.1 Inclusive prompt photon production

The cross section for inclusive prompt photon production, $ep \rightarrow e\gamma X$, has been measured in the following kinematic region: $Q^2 > 35 \text{ GeV}^2$, $E_e > 10 \text{ GeV}$, $139.8^\circ < \theta_e < 171.8^\circ$, $-0.7 < \eta^\gamma < 0.9$ and $5 < E_T^\gamma < 10 \text{ GeV}$, with photon isolation such that at least 90% of the energy found in an $\eta - \phi$ cone of radius 1.0 around the photon is associated with the photon. The measured cross section is

$$\sigma(ep \rightarrow e\gamma X) = 5.64 \pm 0.58(\text{stat.})_{-0.72}^{+0.47}(\text{syst.}) \text{ pb.}$$

The predicted cross sections from PYTHIA and HERWIG are lower than the data by factors of approximately 2 and 8, respectively. Figures 3a and 3b show the measured rapidity and transverse energy distributions, compared to MC predictions normalised to the data. The data are also presented in Table 1. Both PYTHIA and HERWIG describe the E_T^γ spectrum and HERWIG describes the rapidity well. Figure 3c shows the Q^2 distribution of the data, again compared to MC predictions. The agreement of PYTHIA with the data is reasonable, but HERWIG fails to describe the measured Q^2 spectrum. As discussed in Section 6.2, the $O(\alpha^3\alpha_s)$ calculations suggest that the discrepancies between PYTHIA and the data in the rate and photon rapidity distribution may be due to the fact that wide-angle initial- and final-state radiation from the electron are not included in the MC calculations.

6.2 Prompt photon plus jet production

Owing to divergences in cross-section calculations for prompt photons, a comparison to $O(\alpha^3\alpha_s)$ QCD predictions in DIS can be made only when there is a jet accompanying an isolated prompt photon. Jets were reconstructed as described in Section 2. For events satisfying the criteria for isolated prompt photons described above, jets were counted only if they had $E_T^{\text{jet}} > 6 \text{ GeV}$ and $-1.5 < \eta^{\text{jet}} < 1.8$. The measured total cross section for photon plus a single jet within this kinematic region is

$$\sigma(ep \rightarrow e\gamma + \text{jet} + Y) = 0.86 \pm 0.14(\text{stat.})_{-0.34}^{+0.44}(\text{syst.}) \text{ pb.}$$

Figure 4 shows the differential cross sections for ‘prompt photon plus one jet’ events, together with MC predictions. The data are also presented in Table 2. The transverse energies of the photon and the jet are well described by the MC calculations. HERWIG describes the photon rapidity well but the jet pseudorapidity peaks at lower values. PYTHIA describes the jet pseudorapidity well, but the photon rapidity peaks too far forward, as was also the case for inclusive photons.

Figure 5 shows the same data as Fig. 4, compared to the $O(\alpha^3\alpha_s)$ parton-level calculations of Kramer and Spiesberger [12]. These include all possible initial- and final-state single photon and gluon radiation, together with appropriate vertex corrections, and their interference terms. Higher-order effects, such as collinear bremsstrahlung in the same event as a hard non-collinear photon, estimated to be a 4% effect, are omitted. These calculations use the phase-space-slicing method to cancel the infrared and collinear singularities. The MRST parton distributions [28] were used for the parametrisation of the proton structure. Parton-to-photon fragmentation functions were taken from Bourhis, Fontannaz and Guillet [29]. The renormalisation scale was chosen to be the transverse energy of the jet. The effect of changing this scale up or down by a factor of two, to estimate the possible contribution of unknown higher-order terms, is shown in Fig. 5. The predicted total cross section for the mixture of energies and beam charges used in this analysis is 1.33 ± 0.07 pb, where the uncertainty corresponds to the change in the result when the renormalisation scale is varied by a factor of two. This parton-level calculation is compatible with the data.

By definition, the $O(\alpha^3\alpha_s)$ parton-level calculation does not include the effects of hadronisation. Hadronisation effects were investigated by comparing the parton-level PYTHIA and HERWIG distributions with the hadron level. The effect of hadronisation would be to reduce the predictions by 30% to 40%. Because of the overall poor description of the data by the MC simulations, hadronisation corrections were not applied to the $O(\alpha^3\alpha_s)$ calculation.

The $O(\alpha^3\alpha_s)$ calculation shows that 65% of photons are emitted by the electron, concentrated at low photon rapidities, and the rest by quarks. The photon rapidity and jet pseudorapidity distributions for the latter component resemble the PYTHIA predictions, which include only such photons. Interference between these processes contributes only 2% to the total. The transverse-energy distributions of the two processes are similar. The $O(\alpha^3\alpha_s)$ calculation predicts a higher jet cross section at forward pseudorapidity and at low E_T^γ than is seen in the data.

7 Conclusions

The first observation of prompt photon production in deep inelastic scattering has been presented, together with distributions for accompanying jets. Leading-logarithm parton-shower Monte Carlo models for photon emission by quarks (PYTHIA and HERWIG) are each able to describe some but not all of the features of the data. Both describe the transverse energy distribution well and HERWIG describes the photon rapidity well. Both models predict too low a cross section.

The results have been compared to an $O(\alpha^3\alpha_s)$ parton-level calculation for $ep \rightarrow e\gamma + \text{jet} + Y$ in the acceptance region of this measurement. The level of agreement is satisfactory in photon rapidity and jet transverse energy but only fair for photon transverse energy and jet pseudorapidity. The total predicted cross section is consistent with the measured value.

Acknowledgements

We thank the DESY directorate for their strong support and encouragement. The special efforts of the HERA group are gratefully acknowledged. We are grateful for the support of the DESY computing and network services. The design, construction and installation of the ZEUS detector have been made possible by the ingenuity and effort of many people who are not listed as authors. We thank G. Kramer and H. Spiesberger for the $O(\alpha^3\alpha_s)$ calculations. We also thank G. Ingelman and T. Sjöstrand for useful discussions.

References

- [1] E. Anassontzis et al., *Z. Phys. C* **13**, 277 (1982).
- [2] CDF Coll., F. Abe et al., *Phys. Rev. Lett.* **68**, 2734 (1992).
- [3] CDF Coll., F. Abe et al., *Phys. Rev. D* **48**, 2998 (1993).
- [4] CDF Coll., F. Abe et al., *Phys. Rev. Lett.* **73**, 2662 (1994).
- [5] CDF Coll., F. Abe et al., *Phys. Rev. Lett.* **70**, 2232 (1993).
- [6] DØ Coll., S. Abachi et al., *Phys. Rev. Lett.* **77**, 5011 (1996).
- [7] DØ Coll., F. Abbott et al., *Phys. Rev. Lett.* **84**, 2786 (2000).
- [8] ZEUS Coll., J. Breitweg et al., *Phys. Lett. B* **413**, 201 (1997).
- [9] ZEUS Coll., J. Breitweg et al., *Phys. Lett. B* **472**, 175 (2000).
- [10] ZEUS Coll., S. Chekanov et al., *Phys. Lett. B* **511**, 19 (2001).
- [11] A. Gehrmann-De Ridder, G. Kramer and H. Spiesberger, *Nucl. Phys. B* **578**, 326 (2000).
- [12] G. Kramer and H. Spiesberger, private communication.
- [13] ZEUS Coll., M. Derrick et al., *Phys. Lett. B* **297**, 404 (1992).
- [14] M. Derrick et al., *Nucl. Inst. Meth. A* **309**, 77 (1991);
A. Andresen et al., *Nucl. Inst. Meth. A* **309**, 101 (1991);
A. Caldwell et al., *Nucl. Inst. Meth. A* **321**, 356 (1992);
A. Bernstein et al., *Nucl. Inst. Meth. A* **336**, 23 (1993).
- [15] N. Harnew et al., *Nucl. Inst. Meth. A* **279**, 290 (1989);
B. Foster et al., *Nucl. Phys. Proc. Suppl. B* **32**, 181 (1993);
B. Foster et al., *Nucl. Inst. Meth. A* **338**, 254 (1994).
- [16] J. Andruszków et al., Preprint DESY-92-066, DESY, 1992;
ZEUS Coll., M. Derrick et al., *Z. Phys. C* **63**, 391 (1994);
J. Andruszków et al., *Acta Phys. Pol. B* **32**, 2025 (2001).
- [17] ZEUS Coll., S. Chekanov et al., *Eur. Phys. J. C* **21**, 443 (2001).
- [18] ZEUS Coll., J. Breitweg et al., *Eur. Phys. J. C* **1**, 109 (1998).
- [19] T. Sjöstrand et al., *Comp. Phys. Comm.* **135**, 238 (2001).
- [20] G. Marchesini et al., *Comp. Phys. Comm.* **67**, 465 (1992).
- [21] B. Andersson et al., *Phys. Rep.* **97**, 31 (1983).
- [22] B. R. Webber, *Nucl. Phys. B* **238**, 492 (1984).

- [23] R. Brun et al., GEANT3, Technical Report CERN-DD/EE/84-1, CERN, 1987.
- [24] A. Kwiatkowski, H. Spiesberger and H.-J. Möhring, *Comp. Phys. Comm.* **69**, 155 (1992). Also in *Proc. Workshop Physics at HERA*, Ed. W. Buchmüller and G. Ingelman, (DESY, Hamburg, 1991);
H. Spiesberger, *An Event Generator for ep Interactions at HERA Including Radiative Processes (Version 4.6)*, 1996, available on <http://www.desy.de/~hspiesb/heracles.html>.
- [25] H. Spiesberger, *HERACLES and DJANGO: Event Generation for ep Interactions at HERA Including Radiative Processes*, 1998, available on <http://www.desy.de/~hspiesb/djangoh.html>.
- [26] H1 Coll., C. Adloff et al., *Phys. Lett.* **B 517**, 47 (2001).
- [27] ZEUS Coll., S Chekanov et al., *Phys. Lett.* **B 573**, 46 (2003).
- [28] A.D. Martin et al., *Eur. Phys. J.* **C 4**, 463 (1998).
- [29] L. Bourhis, M. Fontannaz and J. P. Guillet, *Eur. Phys. J.* **C 2**, 529 (1998).

η^γ	$d\sigma/d\eta^\gamma$ (pb)
-0.7 to -0.3	$4.95 \pm 0.78^{+0.51}_{-0.63}$
-0.3 to 0.1	$5.20 \pm 0.75^{+0.20}_{-0.42}$
0.1 to 0.5	$2.12 \pm 0.69^{+0.25}_{-0.38}$
0.5 to 0.9	$1.82 \pm 0.66^{+0.24}_{-0.32}$
E_T^γ (GeV)	$d\sigma/dE_T^\gamma$ (pb GeV $^{-1}$)
5.0 to 6.0	$1.25 \pm 0.40^{+0.05}_{-0.03}$
6.0 to 8.0	$1.40 \pm 0.20^{+0.06}_{-0.05}$
8.0 to 10.0	$0.79 \pm 0.10^{+0.10}_{-0.01}$

Table 1: *Differential cross sections for inclusive production of isolated photons with $-0.7 < \eta^\gamma < 0.9$, for $5 < E_T^\gamma < 10$ GeV. The first uncertainty is statistical, the second is systematic.*

η^γ	$d\sigma/d\eta^\gamma$ (pb)	η^{jet}	$d\sigma/d\eta^{\text{jet}}$ (pb)
-0.7 to -0.3	$0.81 \pm 0.20^{+0.39}_{-0.27}$	-1.5 to -0.84	$0.087 \pm 0.043^{+0.059}_{-0.018}$
-0.3 to 0.1	$0.77 \pm 0.19^{+0.33}_{-0.21}$	-0.84 to -0.18	$0.118 \pm 0.068^{+0.20}_{-0.10}$
0.1 to 0.5	$0.16 \pm 0.16^{+0.18}_{-0.17}$	-0.18 to 0.48	$0.47 \pm 0.13^{+0.25}_{-0.10}$
0.5 to 0.9	$0.30 \pm 0.15^{+0.19}_{-0.15}$	0.48 to 1.14	$0.24 \pm 0.10^{+0.10}_{-0.06}$
		1.14 to 1.8	$0.41 \pm 0.12^{+0.10}_{-0.18}$
E_T^γ (GeV)	$d\sigma/dE_T^\gamma$ (pb GeV $^{-1}$)	E_T^{jet} (GeV)	$d\sigma/dE_T^{\text{jet}}$ (pb GeV $^{-1}$)
5.0 to 6.0	$0.136 \pm 0.090^{+0.060}_{-0.043}$	6.0 to 8.0	$0.177 \pm 0.044^{+0.016}_{-0.028}$
6.0 to 8.0	$0.258 \pm 0.050^{+0.069}_{-0.041}$	8.0 to 10.0	$0.132 \pm 0.049^{+0.057}_{-0.022}$
8.0 to 10.0	$0.107 \pm 0.029^{+0.046}_{-0.001}$	10.0 to 12.0	$0.082 \pm 0.032^{+0.068}_{-0.018}$
		12.0 to 16.0	$0.046 \pm 0.031^{+0.023}_{-0.021}$

Table 2: *Differential cross sections for production of isolated photons plus one jet with $-0.7 < \eta^\gamma < 0.9$, for $5 < E_T^\gamma < 10$ GeV and $-1.5 < \eta^{\text{jet}} < 1.8$, for $E_T^{\text{jet}} > 6$ GeV. The first uncertainty is statistical, the second is systematic.*

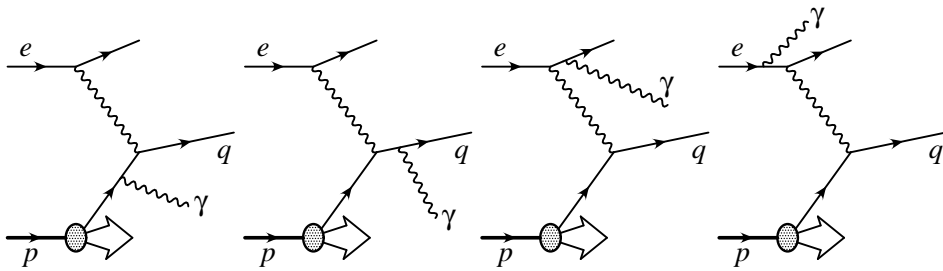


Figure 1: *The lowest-order tree-level diagrams for prompt photon production in ep scattering. Vertex corrections enter at the same order.*

ZEUS

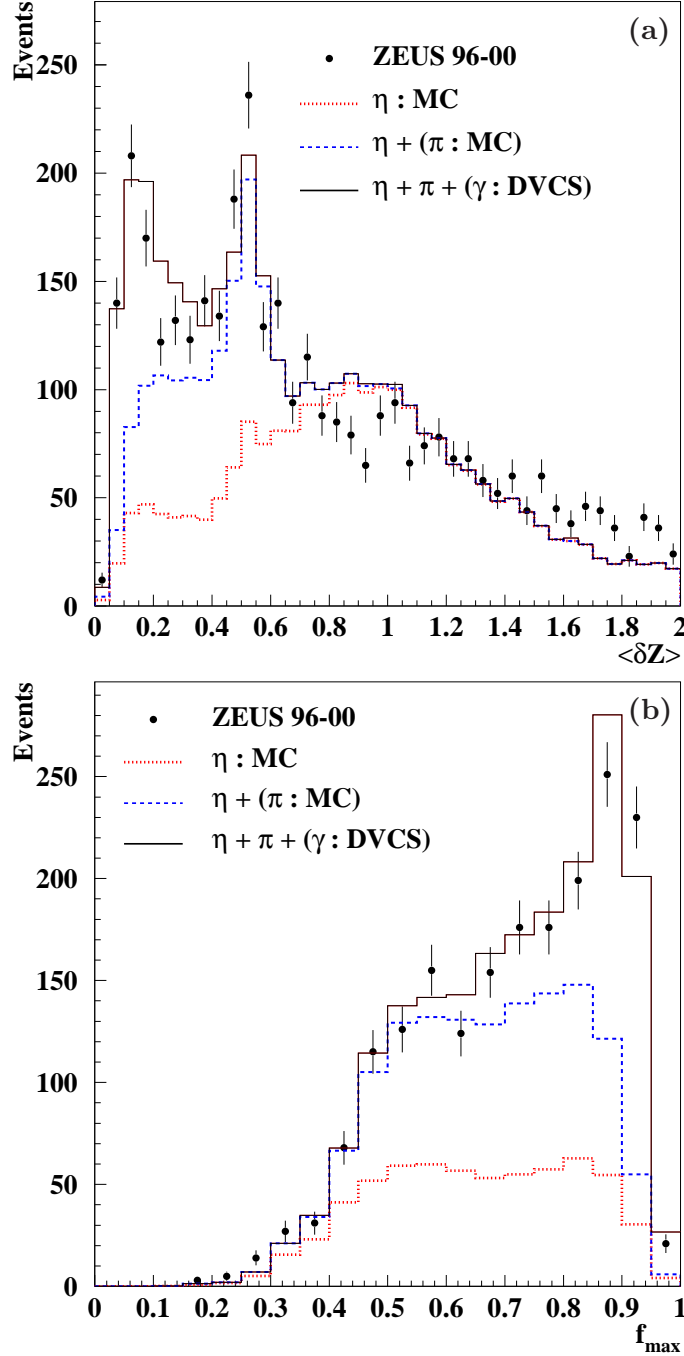


Figure 2: (a) Distribution of $\langle \delta Z \rangle$ for prompt photon candidates in selected events. (b) Distribution of f_{\max} after a cut on $\langle \delta Z \rangle < 0.65$. Also given are fitted distributions for Monte Carlo η mesons, $\pi^0 + \eta$ and $\pi^0 + \eta + \gamma$ (where the γ is taken from DVCS data), with similar selection criteria and E_T^γ spectrum to the observed candidates.

ZEUS

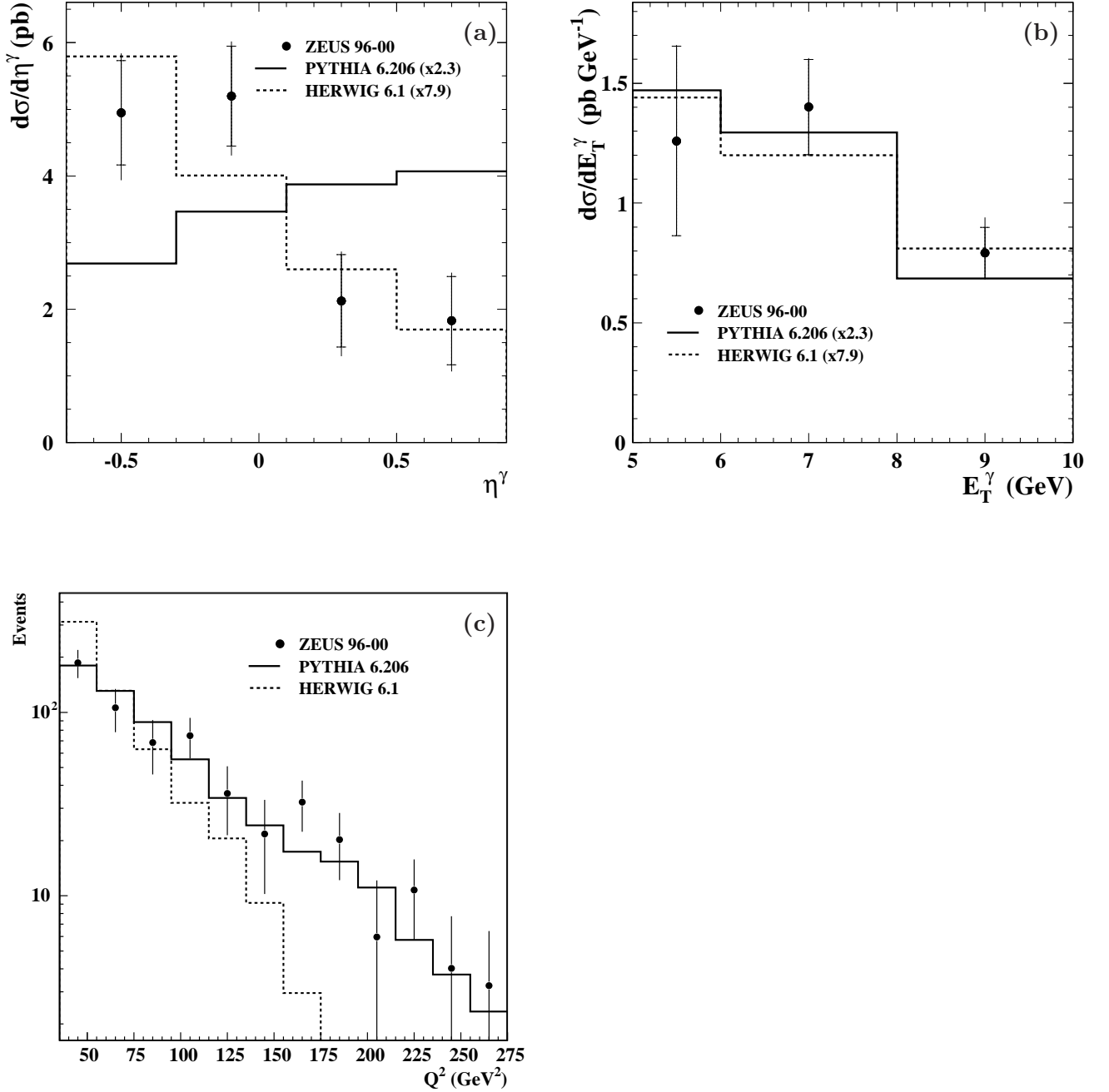


Figure 3: *Inclusive prompt-photon differential cross section (a) in rapidity, (b) in transverse energy, in the range $-0.7 < \eta^\gamma < 0.9$ and $5 < E_T^\gamma < 10$ GeV. The inner error bars are statistical while the outer represent systematic uncertainties added in quadrature. (c) Distribution of Q^2 . In each case the histograms show MC predictions, normalised to data.*

ZEUS

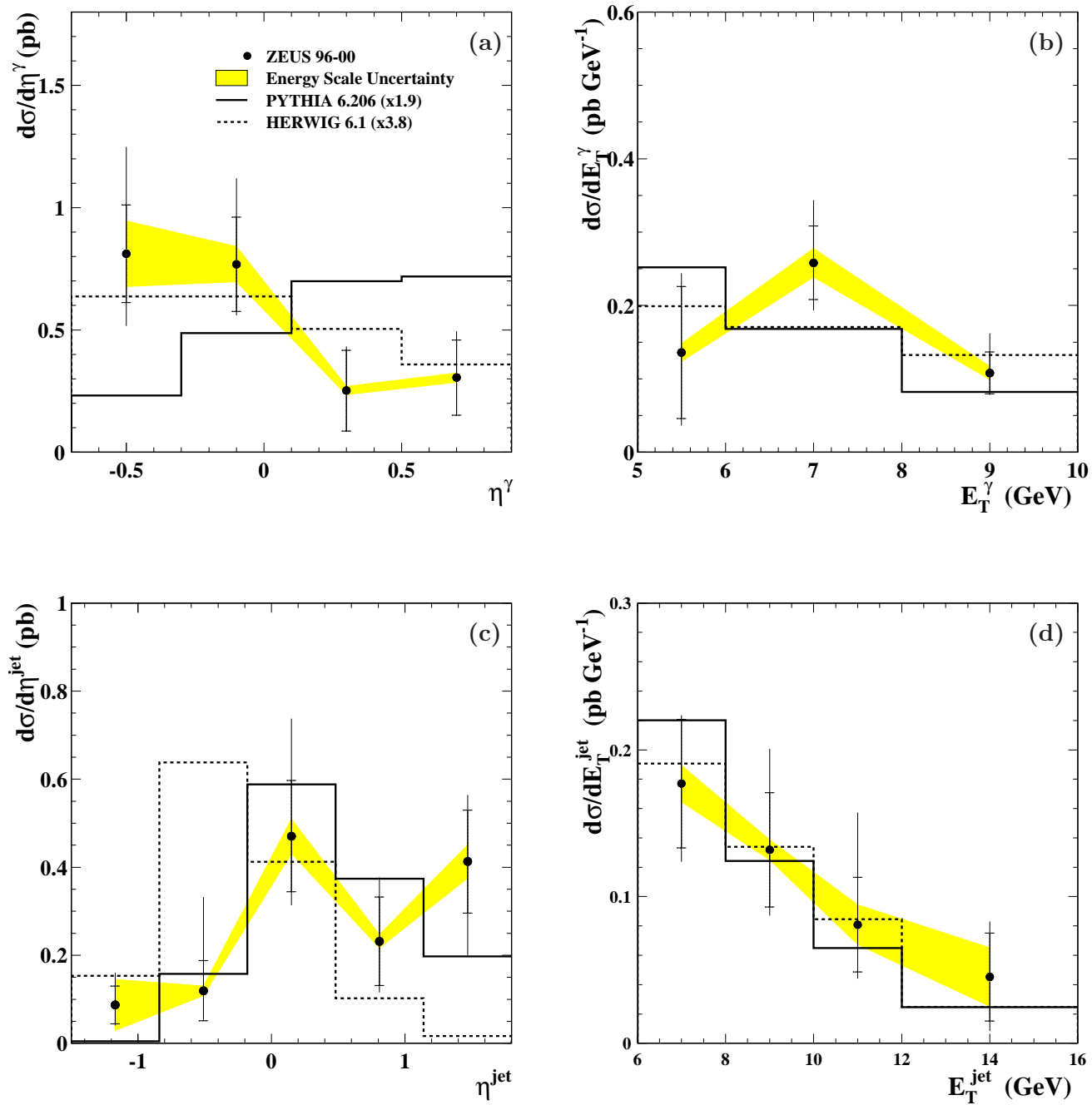


Figure 4: Cross section for prompt-photon-plus-jet production differential in (a) photon rapidity, (b) photon transverse energy, (c) jet pseudorapidity, (d) jet transverse energy, for events with a photon in the range $-0.7 < \eta^\gamma < 0.9$ and $5 < E_T^\gamma < 10$ GeV and one jet in the range $-1.5 < \eta^{\text{jet}} < 1.8$ and $E_T^{\text{jet}} > 6$ GeV. The inner error bars are statistical and the outer represent systematic uncertainties added in quadrature. The band around the data points shows the effect of calorimeter energy-scale uncertainty. The histograms show Monte Carlo predictions, normalised to the data.

ZEUS

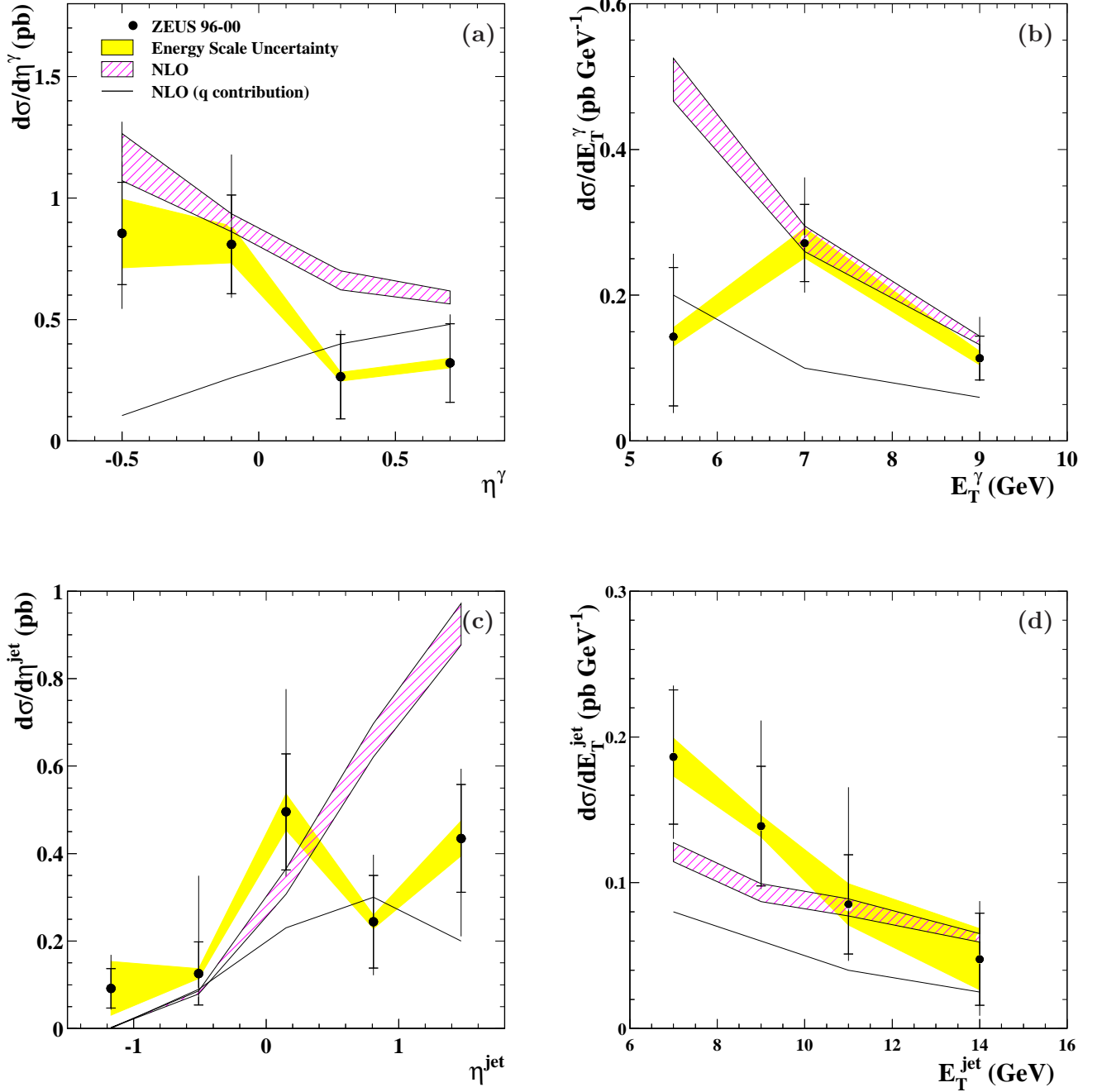


Figure 5: Cross section for prompt-photon-plus-jet production differential in (a) photon rapidity, (b) photon transverse energy, (c) jet pseudorapidity, (d) jet transverse energy, for events with a photon in the range $-0.7 < \eta^\gamma < 0.9$ and $5 < E_T^\gamma < 10$ GeV and one jet in the range $-1.5 < \eta^{\text{jet}} < 1.8$ and $E_T^{\text{jet}} > 6$ GeV. The inner error bars are statistical while the outer represent systematic uncertainties added in quadrature. The band around the data points shows the effect of calorimeter energy scale uncertainty. The boxed band shows the parton-level predictions of Kramer and Spiesberger including the effect of renormalisation scale uncertainty. The single line indicates their prediction of the contribution of photons radiated from the quark line.